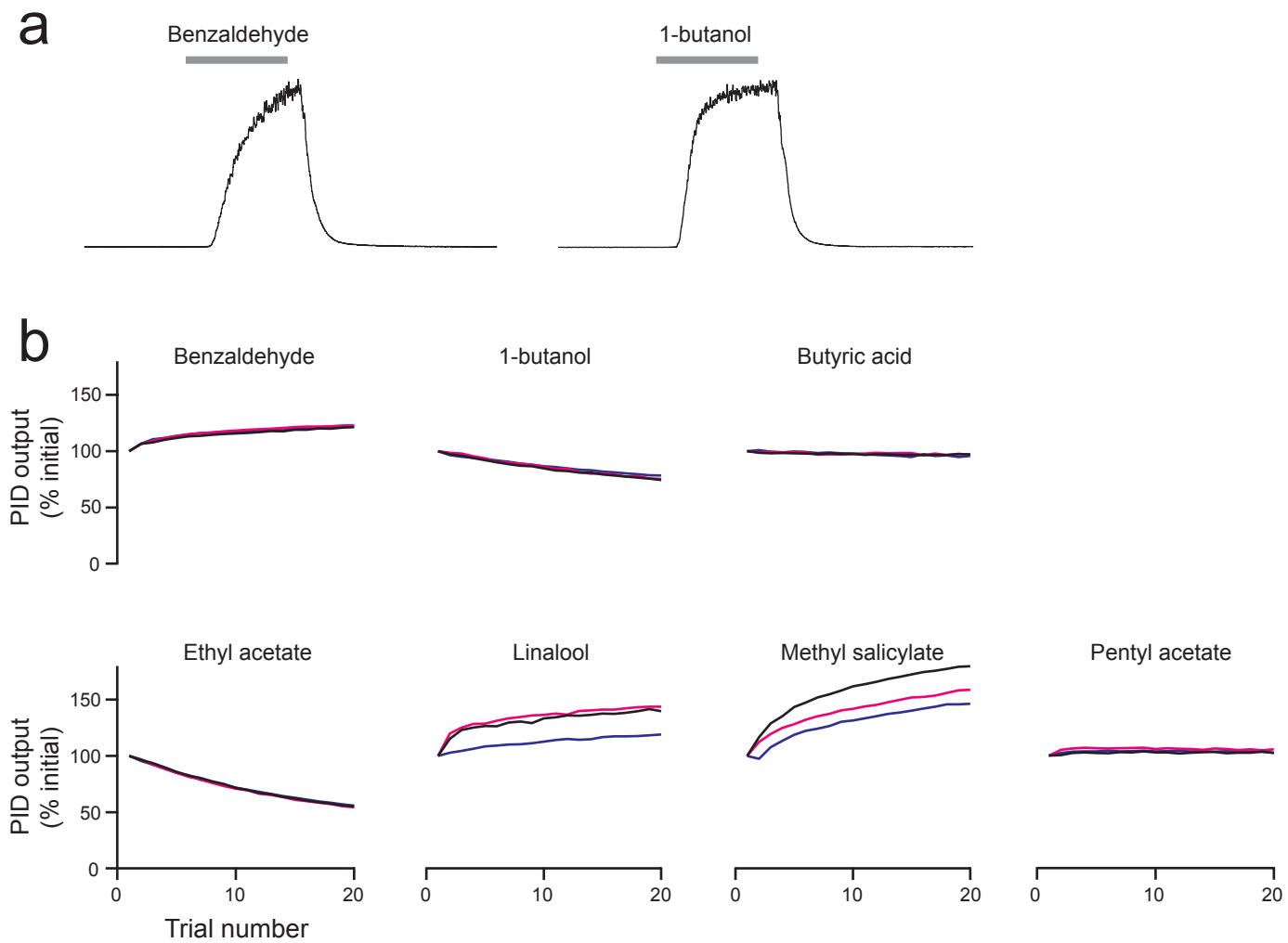


Supplementary Figure 1

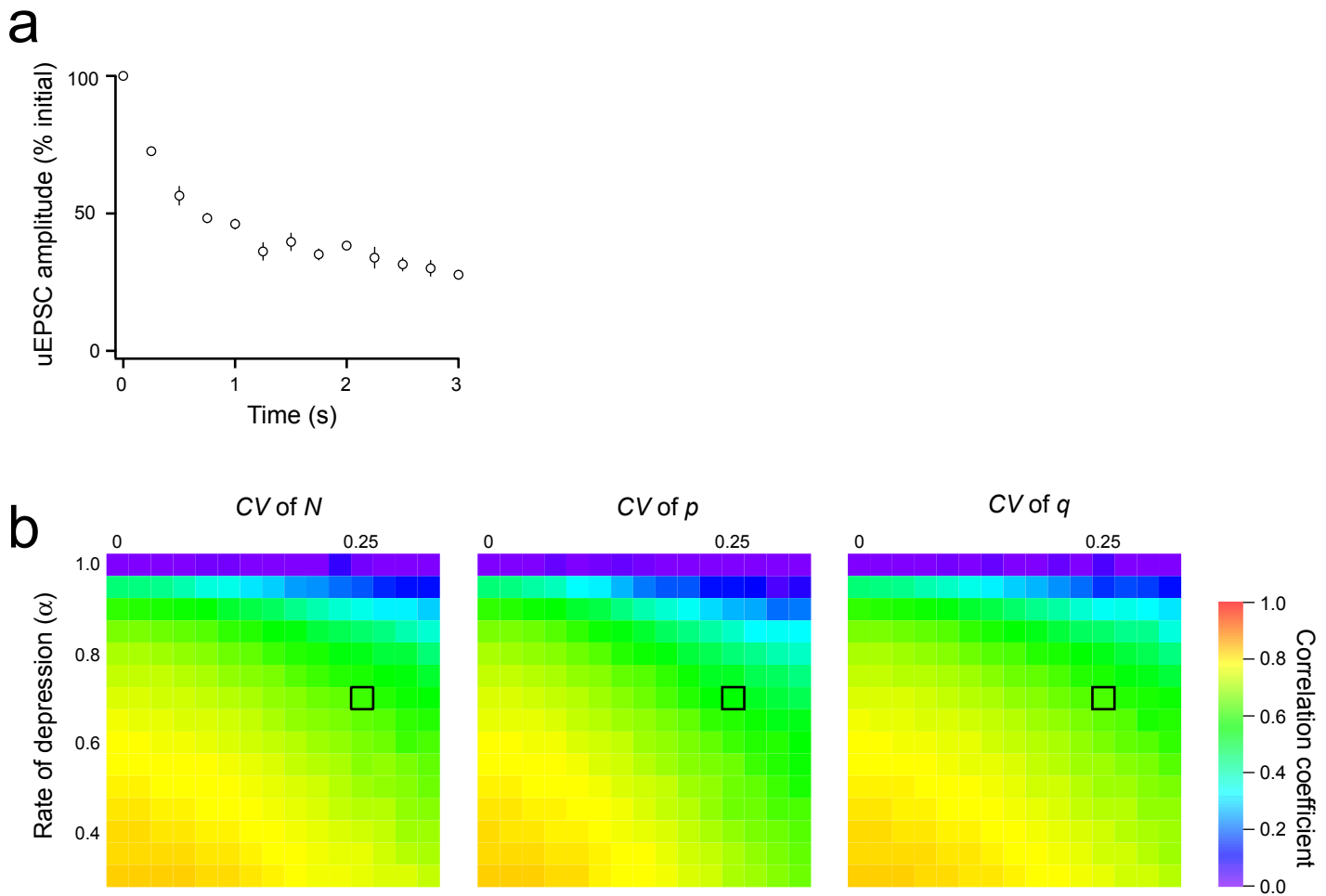


Supplementary Fig. 1 Trial-to-trial variability of olfactory stimuli is low.

(a) Representative output of a photoionization detector (PID, Aurora Scientific, MiniPID) in response to a 500-ms odor pulse. The amplitude is scaled and shown in arbitrary units.

(b) The PID response was integrated over the 500-ms stimulation period and plotted over 20 consecutive trials. Odors were applied every 40 s. The results of three experiments are shown in different colors. Note that trial-to-trial variability is very low with an average coefficient of variation of 0.015 ± 0.003 (comparisons of consecutive trials only). This indicates that variation in the stimulus has little contribution to the variation we observe in neural responses on a trial-to-trial basis. In this study, all shift-corrections of cross-covariance were computed using consecutive trials (see Methods). This minimizes the impact of gradual changes in the stimulus (e.g., the rundown of ethyl acetate).

Supplementary Figure 2

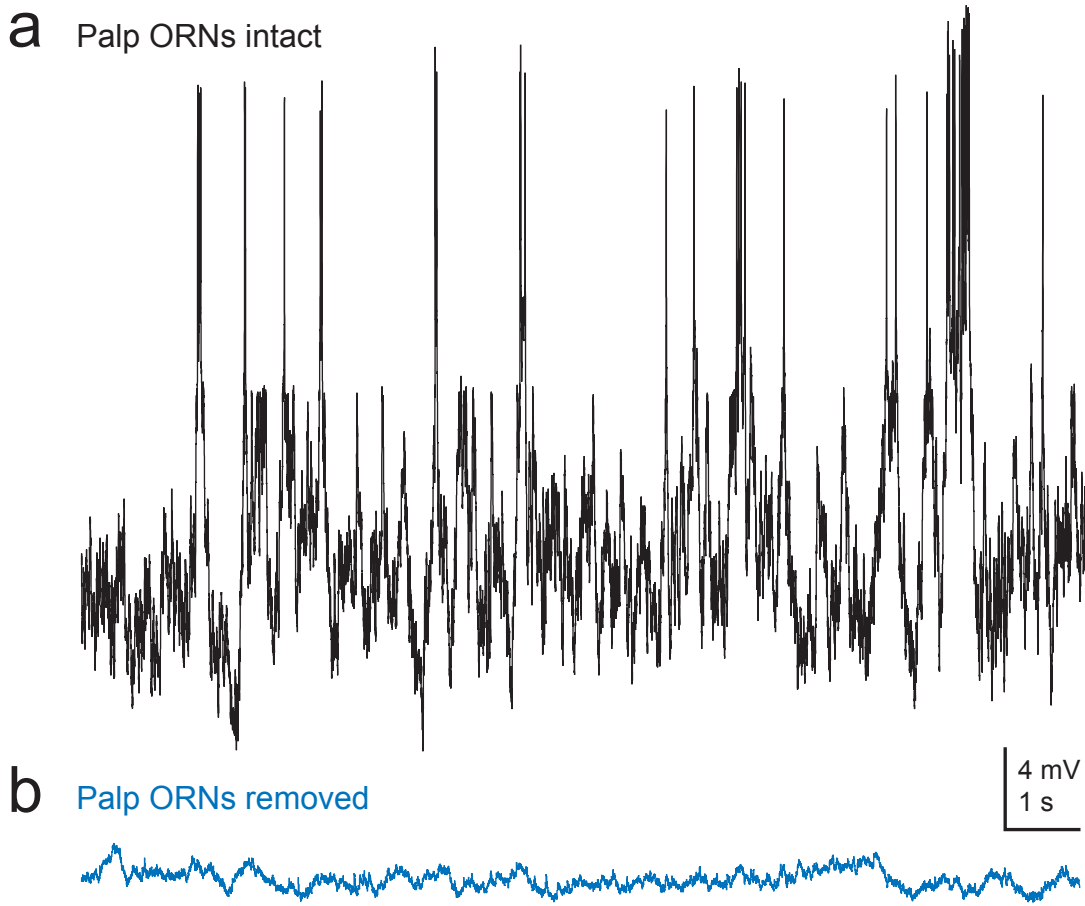


Supplementary Fig. 2 Short-term depression and its impact on the correlation between simulated EPSC amplitudes in a divergent feedforward circuit.

(a) Experimental data used to constrain our simulation of short-term depression. A single ORN axon directly presynaptic to the recorded DM4 PN was stimulated using a minimal stimulation protocol (Kazama and Wilson, 2008). The unitary EPSC amplitude depressed smoothly and rapidly during 4 Hz stimulation ($n = 3$, error bars are s.e.m.). This is consistent with the fact that each ORN-PN synapse corresponds to many vesicular release sites, each with a high probability of release (Kazama and Wilson, 2008). We used least-squares regression on the means of this dataset to obtain α and τ (see Methods).

(b) Trial-averaged unitary EPSC amplitude varies somewhat across experiments. For glomerulus DM4, the coefficient of variation (CV) across experiments is 0.25 (Kazama & Wilson 2008). We incorporated this variation into our simulation by randomly drawing synaptic parameters (N , p , or q) from a normal distribution with this CV. Here we show that the results of our simulation are robust to the magnitude and source of this variation. Spontaneous EPSCs were simulated in pairs of PNs (as described in Fig. 6 and Methods) and the mean correlation coefficient (color scale) between amplitudes was computed across all synchronous EPSCs. The simulation was repeated for a range of values for α (the rate of depression) and a range of values for the CV. This variation was modeled as a variation in N , initial p , or q . Values boxed in black correspond to conditions that best match the data. Overall, a high level of correlation was observed under a wide range of values, meaning that this phenomenon is robust within this range.

Supplementary Figure 3

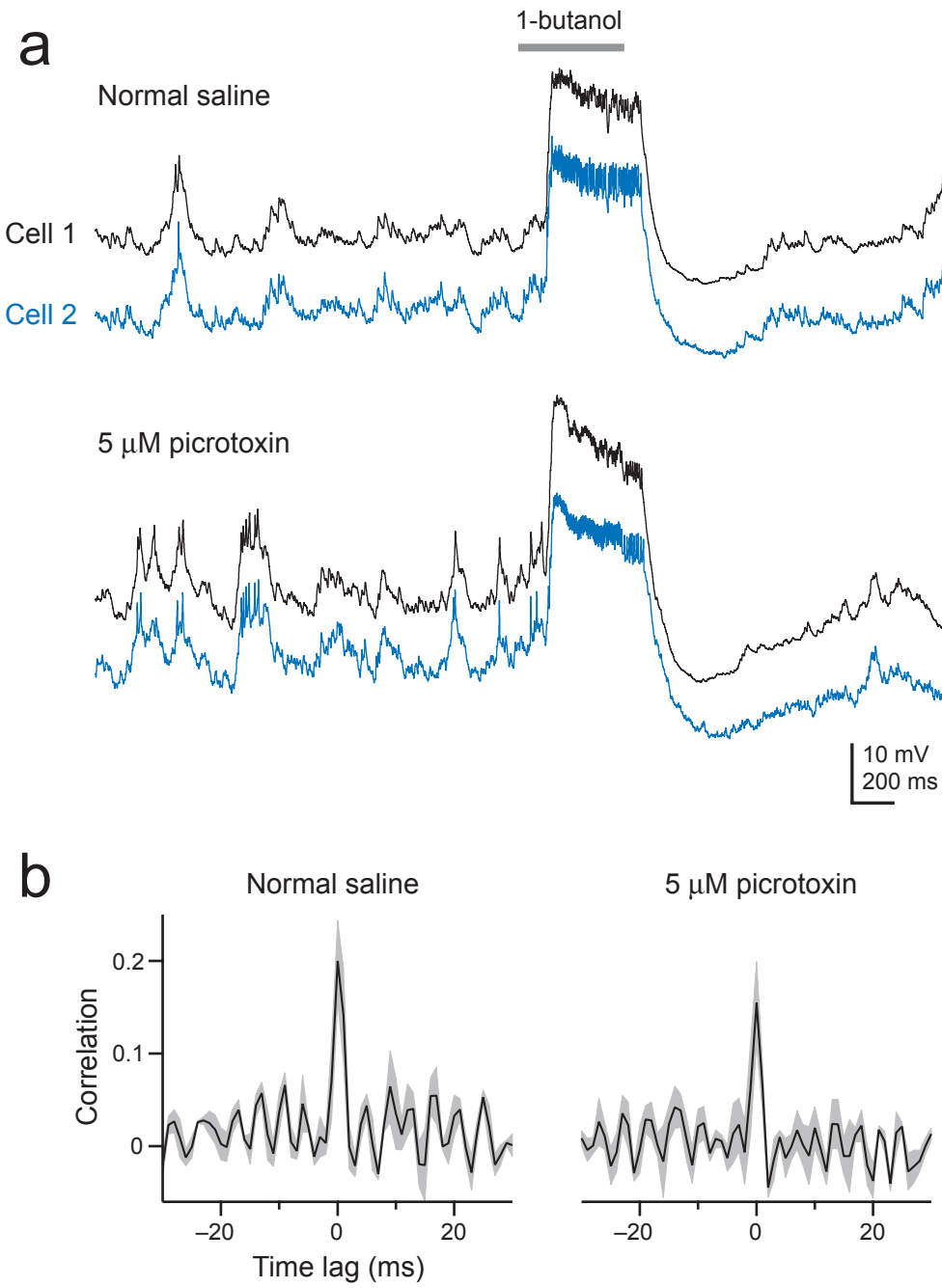


Supplementary Fig. 3 Spontaneous fluctuations in membrane potential are mainly driven by direct ORN input, not central input.

(a) Whole-cell current-clamp recording made from a palp PN (glomerulus VM7) in a fly with both palps and antennae intact. Note large spontaneous EPSPs, some of which trigger spontaneous action potentials.

(b) Whole-cell current-clamp recording made from a palp PN (glomerulus VM7) in a palp-less but otherwise intact fly. Because direct ORN inputs have been selectively removed, membrane potential fluctuations mainly reflect fluctuations in central input (via local interneurons and PN-PN connections), as well as events intrinsic to this PN. Note that the magnitude of fluctuations is much smaller without direct ORN input. Thus, the major source of noise under these conditions is direct ORN input; although central input to homotypic PNs is highly correlated, the fluctuations arising from central inputs are comparatively small, and so their role in producing correlated fluctuations in spike timing should be relatively small.

Supplementary Figure 4



Supplementary Fig. 4 Noise correlation is insensitive to a GABA_A receptor antagonist.

(a) Recordings from a pair of homotypic ipsilateral PNs in glomerulus DM6 with or without 5 μ M picrotoxin. This concentration of picrotoxin is effective at blocking GABA_A receptors in Drosophila neurons (Su, H. & O'Dowd, D. K. J. Neurosci. 23, 9246-9253 (2003); Wilson, R. I. & Laurent, G. J. Neurosci. 25, 9069-79 (2005)). Gray bar indicates 500 ms period of odor application.

(b) Spike correlation is largely unaffected by 5 μ M picrotoxin ($n = 3$; $p = 0.66$, paired t -test). Gray shade indicates \pm s.e.m.

Supplementary Methods

Fly stocks. Flies were raised on conventional cornmeal agar under a 12-h light/12-h dark cycle at 25 °C. All experiments were performed on adult female flies, 2-5 days post-eclosion. Stocks were kindly provided as follows: *NP3062-Gal4* and *NP7217-Gal4* (Kei Ito and Liqun Luo)¹; *Or59b-Gal4* (X) (Barry J. Dickson)². *UAS-CD8:GFP* (X) and *UAS-nls:GFP* (II) are available from the Bloomington stock center.

PN recordings. The internal patch-pipette solution used for voltage-clamp recordings contained (in mM): 140 cesium aspartate, 10 HEPES, 4 MgATP, 0.5 Na₃GTP, 1 EGTA, 1 KCl, 13 biocytin hydrazide, and 10 QX-314 chloride (Alomone Labs). The pH of the internal solution was adjusted to 7.3 and the osmolarity was adjusted to ~ 265 mOsm. For current-clamp experiments, QX-314 was removed and cesium was replaced with an equal concentration of potassium. External saline contained (in mM): 103 NaCl, 3 KCl, 5 *N*-tris(hydroxymethyl) methyl-2-aminoethane-sulfonic acid, 8 trehalose, 10 glucose, 26 NaHCO₃, 1 NaH₂PO₄, 1.5 CaCl₂, and 4 MgCl₂ (osmolarity adjusted to 270-275 mOsm). The saline was bubbled with 95% O₂/5% CO₂ and reached a pH of 7.3. Recordings were acquired with an Axopatch 200A amplifier (Axon Instruments) equipped with a CV 201A headstage (500 MΩ) and an Axopatch 1D amplifier (Axon Instruments) equipped with a CV-4 headstage (500 MΩ). In most cases, only one pair of neurons was recorded per brain. Immunohistochemistry was performed as described previously³ except that in the secondary incubation we used 1:250 goat anti-mouse:Alexa Fluor 633 and 1:1000 streptavidin:Alexa Fluor 568 (Invitrogen). The nc82 antibody used to outline glomerular boundaries was obtained from the Developmental Studies Hybridoma Bank (U. of Iowa).

Olfactory stimulation. All odors were diluted 100-fold in paraffin oil, and the headspace of the vial containing this solution was further diluted 10-fold in air. The flow rate of the odor delivery stream was 2.2 L/min. The end of the odor delivery tube was 3.2 mm (i.d.) and it was positioned 8 mm from the fly. Odors were delivered with a custom-built olfactometer as described previously^{4, 5}. Stimuli were applied for 500 ms every 40 s for 10-80 times (typically 15-20 times) per stimulus.

Data analysis. All analyses were performed in Igor Pro using custom software. All mean values are reported as mean \pm s.e.m., averaged across experiments. Spontaneous EPSCs were detected and their amplitudes were calculated using a previously described algorithm⁶. The percentage of spikes that are synchronous in a pair of PN recordings was computed using the raw cross-correlogram (the histogram of spikes in cell A at time delays relative to a spike in cell B) after shift correction (subtraction of the cross-correlogram created from the spikes in cell A on the i th trial relative to spikes in cell B on the $(i + 1)$ th trial). The percentage of synchronous spikes is the integral of the cross-correlogram (in a window 1.6 ms wide, centered around lag zero), normalized by the total number of spikes in cell B. The shift correction removes correlations expected by chance based on each cell's average firing rate and the stimulus itself. This metric has also been termed correlation strength⁷. An integration window of 1.6 ms was chosen because it contains most of the peak in the shift-corrected cross-correlogram.

Morphological analysis. The distance between the nearest axonal processes belonging to different homotypic ipsilateral PNs (Fig. 8d) was calculated using ImageJ (NIH) and MATLAB (The MathWorks). Confocal sections of ipsilateral DM6 PNs labeled with different Alexa Fluor dyes were binarized using a threshold common to all the z -sections. Only the boutons were

selected as a region of interest (ROI) in the mushroom body because vesicular release sites are reportedly present along the perimeter of boutons but not along the primary axon in the antennocerebral tract or thin axons connecting the primary axon and boutons⁸. On the other hand, all the axonal nerve endings were selected as a ROI in the lateral horn because synaptic vesicular markers are uniformly and continuously distributed throughout the axons in this brain region⁸. Because synapses are made only on the surface of axonal processes, the voxels on the perimeter of the objects were extracted as a ROI. The distance between a voxel occupied by one cell and the nearest voxel occupied by the other cell was calculated for every voxel. These procedures were conducted separately in the mushroom body and the lateral horn.

References for Supplementary Methods:

1. Kazama, H. & Wilson, R. I. Homeostatic matching and nonlinear amplification at identified central synapses. *Neuron* 58, 401-13 (2008).
2. Couto, A., Alenius, M. & Dickson, B. J. Molecular, anatomical, and functional organization of the Drosophila olfactory system. *Curr. Biol.* 15, 1535-47 (2005).
3. Wilson, R. I. & Laurent, G. Role of GABAergic inhibition in shaping odor-evoked spatiotemporal patterns in the Drosophila antennal lobe. *J. Neurosci.* 25, 9069-79 (2005).
4. Bhandawat, V., Olsen, S. R., Schlief, M. L., Gouwens, N. W. & Wilson, R. I. Sensory processing in the Drosophila antennal lobe increases the reliability and separability of ensemble odor representations. *Nat. Neurosci.* 10, 1474-82 (2007).
5. Olsen, S. R., Bhandawat, V. & Wilson, R. I. Excitatory interactions between olfactory processing channels in the Drosophila antennal lobe. *Neuron* 54, 89-103 (2007).
6. Kudoh, S. N. & Taguchi, T. A simple exploratory algorithm for the accurate and fast detection of spontaneous synaptic events. *Biosens. Bioelectron.* 17, 773-82 (2002).
7. Dan, Y., Alonso, J. M., Usrey, W. M. & Reid, R. C. Coding of visual information by precisely correlated spikes in the lateral geniculate nucleus. *Nat. Neurosci.* 1, 501-7 (1998).
8. Jefferis, G. S. et al. Comprehensive maps of Drosophila higher olfactory centers: spatially segregated fruit and pheromone representation. *Cell* 128, 1187-203 (2007).